ACS APPLIED MATERIALS & INTERFACES

Research Article

www.acsami.org

Enhanced Uptake and Selectivity of CO_2 Adsorption in a Hydrostable Metal–Organic Frameworks via Incorporating Methylol and Methyl Groups

Chao Wang,[†,‡] Liangjun Li,[§] Sifu Tang,[†] and Xuebo Zhao*[,†,§]

[†]Qingdao Institute of Bioenergy and Bioprocess Technology, Chinese Academy of Sciences, Qingdao 266101, People's Republic of China

[‡]University of Chinese Academy of Sciences, Beijing 100049, People's Republic of China

[§]Research Institute of Unconventional Petroleum and Renewable Energy, China University of Petroleum (East China), Qingdao 266580, People's Republic of China

Supporting Information

ABSTRACT: A new methylol and methyl functionalized metal–organic frameworks (MOFs) QI-Cu has been designed and synthesized. As a variant of NOTT-101, this material exhibits excellent CO_2 uptake capacities at ambient temperature and pressure, as well as high CH_4 uptake capacities. The CO_2 uptake for QI-Cu is high, up to 4.56 mmol g^{-1} at 1 bar and 293 K, which is top-ranked among MOFs for CO_2 adsorption and significantly larger than the nonfunctionalized NOTT-101 of 3.93 mmol g^{-1}. The enhanced isosteric heat values of CO_2 and CH_4 adsorption were also obtained for this linker functionalized MOFs. From the single-component adsorption isotherms, multicomponent adsorption was predicted using the ideal adsorbed solution theory (IAST). QI-Cu shows an improvement in adsorptive selectivity of CO_2 over CH_4 and N_2 below 1 bar. The incorporation of methylol and methyl groups also greatly improves the hydrostability of the whole framework.

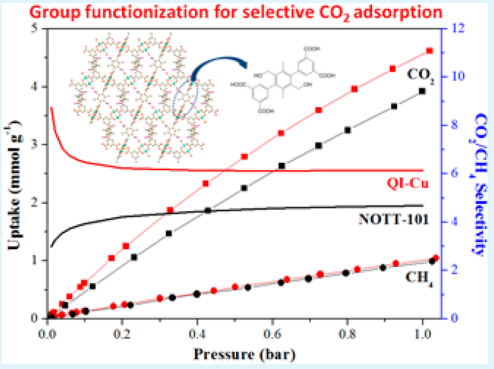

KEYWORDS: *metal–organic frameworks (MOFs), CO_2 uptake, selectivity, functionalization*

1. INTRODUCTION

The Earth's carbon cycle is seriously perturbed by human activities associated with the elevated carbon dioxide (CO_2) concentration in the atmosphere, ocean and soil.[1] In the face of the resulting climate changes,[2,3] therefore, it is imperative to develop effective ways to mitigate this intense situation. Compared with the chemical activation of CO_2 solutions,[4,5] CO_2 capture exhibits greater efficiency at anthropogenic point sources, such as natural gas-fired power plants.[6−8] Solid porous adsorbent materials, including both physisorbents and chemisorbents,[8,9] have been widely investigated due to their favorable adsorption capacity, high thermostability and low energy costs of regeneration compared with conventional amine solutions.[6,10] In addition to these performance parameters, the selectivity toward CO_2 plays a critical role for any CO_2 capture material.[8,11]

Metal–organic frameworks (MOFs)[12,13] are a subclass of coordination polymers that show great potential for applications of CO_2 storage and sequestration[6,14,15] due to their prodigious surface area[16−18] and tunable functional pore environment.[19−22] A high capacity for storage of CO_2 can be achieved by various approaches including appropriate design of framework structure,[23] organic groups functionalization[24,25] and postsynthesis modification.[26,27] However, an unavoidable case is that the selectivity of CO_2 over other gases drops off significantly with increasing loadings, which is not conducive to practical applications of CO_2 separations.[28] Furthermore, enhancing the CO_2 uptake at mild conditions, such as ambient temperature and pressure, is also a critical factor for future industrial applications.

The NOTT series of MOF materials are very impressive in their H_2 and CH_4 adsorption properties.[29−31] To date, some studies have reported the functionalization of the parent NOTT series materials, including tuning the moisture and thermal stability and introduction of mesopores.[32,33] However, it appears to be almost ignored that the MOFs exhibit excellent CO_2 adsorption properties, especially under ambient temperature and pressure. The incorporation of polar groups like amino or hydroxy into the organic linkers is more favorable for the enhancement of CO_2 uptake through increasing interactions of CO_2 molecules with the framework of MOFs, and a higher selectivity of CO_2 upon other permanent gases may be achieved thereupon.[6,14,15,34] Furthermore, some studies have reported that the addition of nonpolar groups, such as methyl, is an effective way to tune the CO_2 Henry's coefficient and provide an increase in CO_2 uptake at a low pressure.[35] On the

Received: July 9, 2014
Accepted: September 8, 2014
Published: September 8, 2014

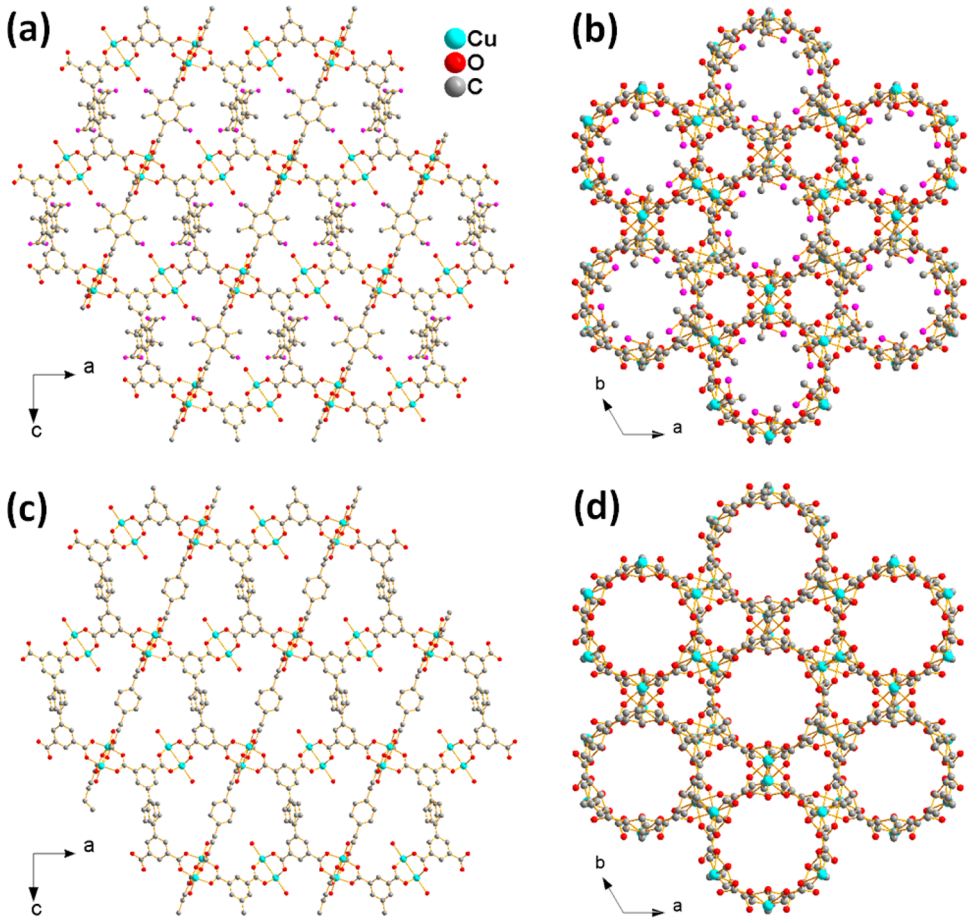

Figure 1. Comparisons of the structures of (a,b) QI-Cu and (c,d) NOTT-101 along *b*- and *c*-axis (the O atoms in hydroxy groups are shown as pink spheres and the H atoms are omitted for clarity).

basis of the above considerations, we selected NOTT-101 as an exemplar of the series of MOFs and synthesized a functionalized variant QI-Cu via incorporating both of methylol and methyl into the linker. Despite the loss of surface area and pore volume, QI-Cu exhibits higher CO_2 and CH_4 uptake capacities than NOTT-101 in the low pressure region, revealing the stronger gas affinity in QI-Cu caused by the incorporation of methylol and methyl groups, which is consistent with the greater isosteric heat of adsorption for QI-Cu. Furthermore, gas selectivities were calculated for QI-Cu and NOTT-101 through Henry's law and ideal adsorbed solution theory (IAST), respectively. The results indicated that grafting methylol and methyl on the linker may be a promising approach for enhancing adsorptive selectivity of CO_2 over other gases in MOFs. Moreover, the hydrostability for QI-Cu was highly enhanced by linker functionalization.

2. EXPERIMENTAL SECTION

2.1. Materials. All reagents and solvents were commercially available and used without further purification. 3,5-Dimethylphenylboronic acid (≥95%), *p*-xylene (≥99%) and tetrakis(triphenylphosphine)palladium ($Pd(PPh_3)_4$) (≥99.99%) were purchased from Sigma-Aldrich. *Tert*-butanol (^tBuOH) (≥98.0%), copper(II) nitrate trihydrate ($Cu(NO_3)_2{\cdot}3H_2O$) (99.0%−102.0%), potassium permanganate ($KMnO_4$) (≥99.5%), methanol (MeOH) (≥99.5%), ethanol (EtOH) (≥99.7%), trichloromethane ($CHCl_3$) (≥99.0%), tetrahydrofuran (THF) (≥99.0%), 1,4-dioxane (≥99.5%), *N*,*N*-dimethylacetamide (DMA) (≥99.0%), bromine (Br_2) (≥99.5%), iodine (I_2) (≥99.8%), sulfuric acid (H_2SO_4) (95.0%−98.0%), hydrochloride acid (HCl) (36.0%−38.0%), nitric acid (HNO_3) (65.0%−68.0%), sodium hydroxide (NaOH) (≥96.0%), sodium sulfate anhydrous (Na_2SO_4) (≥99.0%), potassium phosphate (K_3PO_4) (≥97.0%) and paraformaldehyde (≥95.0%) were purchased from Sinopharm Chemical Reagent Co., Ltd. Hydrobromic acid 33 wt % solution in acetic acid (HBr/HOAc) was purchased from J&K Scientific Ltd. High purity (99.999%) gases of nitrogen, methane and carbon dioxide and gas mixtures (CO_2/CH_4 and CO_2/N_2) were provided by Qingdao Heli Gas Co., Ltd., China.

2.2. Syntheses of the Ligand and MOFs. The ligand of benzene-1,3-dicarboxyethylester-5-boronic acid (H_4L^1) and the intermediate products of 3,5-dicarboxyethylester-phenylboronic acid and 3,5-dicarboxyethylester-phenylboronic acid were synthesized using the literature method.[29]

Synthesis of 1,4-Bis(bromomethyl)-2,5-dimethylbenzene. *p*-Xylene (10.62 g, 0.10 mol) and paraformaldehyde (6.00 g, 0.20 mol) were added into 60 mL of HBr/HOAc (33 wt %) aqueous solution, and the solution was stirred at 85 °C until a white solid precipitate was observed. The solution was kept at 85 °C for 20 min and then heated to 95 °C for 12 h. 100 mL of deionized water was added into the above solution. The resulting product obtained after filtration was washed with deionized water and air-dried at 65 °C (25.90 g, 88% yield).

Synthesis of 1,4-Dibromo-2,5-bis(bromomethyl)-3,6-dimethylbenzene. 1,4-Bis(bromomethyl)-2,5-dimethylbenzene (5 g, 0.017 mol) was dissolved in 50 mL of CH_2Cl_2 and three I_2 particles (~0.05 g) were added into the solution. After that, 20 mL of liquid Br_2 was added into the solution dropwise and then the solution was stirred under reflux for 2 h at room temperature and 1 h at 50 °C. NaOH aqueous solution (1 M) was added to remove the excess liquid Br_2. The white precipitate was collected by filtration, washed with water

and then dried under vacuum at 65 °C (6.34 g, 82% yield). The obtained white solid was hydrolyzed with NaOH (6 g, 0.15 mol) in THF/EtOH/H_2O (5/2/6, 130 mL) solution and acidified with concentrated HCl to afford the white participate (3.77 g, 83% yield)

Synthesis of 2,5-Bis(hydroxymethyl)-3,6-dimethyl-1,4-diisophthalic Acid (H_4L^2). 1,4-Dibromo-2,5-bis(bromomethyl)-3,6-dimethylbenzene (2.45 g, 7.56 mmol), 3,5-dicarboxyethylester-phenylboronic acid (4.44 g, 16.7 mmol) and K_3PO_4 (21.0 g, 100 mmol) were combined in a 500 mL flask and degassed at the Schlenk line and filled with argon. $Pd(PPh_3)_4$ (0.50 g, 0.43 mmol) and dioxane (300 mL) were introduced into the flask under argon atmosphere and the mixture was heated with stirring at 95 °C for 72 h. After the solution was cooled to room temperature, the solvent was removed under reduced pressure, and the resulting gray solid was extracted using $CHCl_3$ for three times. The extraction was washed with water and dried with anhydrous Na_2SO_4. The obtained white solid was hydrolyzed with NaOH (12 g, 0.30 mol) in THF/EtOH/H_2O (2/2/3, 250 mL) solution and acidified with concentrated HCl to afford the white participate (2.6 g, 70% yield). ^{1}HNMR (600 MHz, DMSO-d_6, ppm): 13.36 (b, 4H), 8.53 (t, 2H), 7.96 (d, 4H), 3.99 (s, 4H), 3.02 (s, 2H), 2.01 (s, 6H).

Syntheses of MOFs. As for QI-Cu, a mixture of the organic ligand H_4L^2 (0.10 mmol) and $Cu(NO_3)_2{\cdot}3H_2O$ (0.20 mmol) and a mixed solvent (DMA/H_2O/HNO_3, 9/3/1 mL) were placed in a Telfon-lined stainless steel autoclave (20 mL) and heated at 100 °C for 3 days. $[Cu(C_{13}H_7O_5)(H_2O)]{\cdot}1.5DMA{\cdot}0.5H_2O$: yield, 60 mg (64%) based on H_4L^2. Elemental analysis for $C_{90}H_{87}N_3Cu_2O_{36}$ (M_r = 956.87) (%) calcd: H 5.51, C 48.92, N 4.50. Found: H 5.58, C 48.57, N 4.68. NOTT-101 was synthesized using the same experimental procedure as QI-Cu except that the ligand H_4L^2 was replaced by H_4L^1.

2.3. Characterizations. ^{1}H NMR spectra were recorded on a Bruker AVANCE III (600 MHz) spectrophotometer. The C, H and N analyses were performed on an Elementar Vario EL III elemental analyzer. Powder X-ray diffraction (PXRD) measurements were carried using a Bruker axs D8 ADVANCE $\theta/2\theta$ diffractometer equipped with Cu Kα (λ = 1.5418 Å), with a scan speed of 2° min^{-1} and a step size of 0.02° in 2θ at room temperature. Single-crystal X-ray diffraction data were collected on a Bruker Smart CCD diffractometer using a ω-scan method with graphite monochromated Mo Kα radiation (λ = 0.710 73 Å) at 173 K. Absorption corrections were collected using a multiscan technique. The structures were solved by direct methods and developed by difference Fourier techniques using the SHELXTL[36] software package. The SQUEEZE program implemented in PLATON[37] was used to remove the highly disordered guest molecules in QI-Cu. Thermogravimetric analysis (TGA) was performed in the temperature range 20−800 °C on a NETZSCH STA449 F3 TG-DSC analyzer under a flow of nitrogen (20 mL/min) at a ramp rate of 10 °C/min. Gas sorption isotherms were measured using an intelligent gravimetric analyzer (IGA-001, Hiden Isochema, Warrington, UK). The system is an ultrahigh vacuum (UHV) system consisting of a fully computer controlled microbalance with both pressure and temperature regulation systems. The microbalance had a long-term stability of ±1 μg with a weighing resolution of 0.2 μg. The pressure transducers had ranges of 0−0.1 MPa. Nitrogen sorption isotherms were performed at 77 K using a cryogenic liquid nitrogen bath over the pressure range of 0−1 bar. Gas sorption isotherms between 273 and 303 K were obtained using a circulating water−ethylene glycol bath controlled by a computer using IGA software. The sample temperature was measured using a thermocouple located 5 mm from the sample. The sample was outgassed to constant weight at <10^{-6} Pa and 373 K prior to commencing adsorption measurements. The weights of activated NOTT-101 sample for gas adsorption measurement were 22.10 and 28.05 mg for single-component and multicomponent adsorption, respectively. The weights of activated QI-Cu sample for gas adsorption measurement were 85.71 and 126.55 mg for single-component and multicomponent adsorption, respectively.

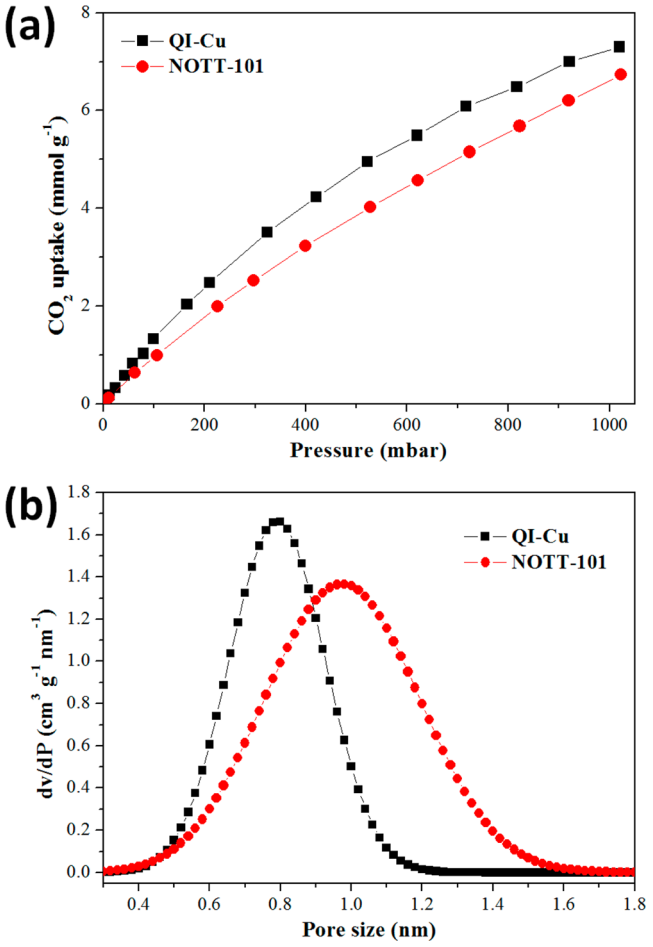

Figure 2. (a) CO_2 dsorption isotherms of at 273 K one QI-Cu and NOTT-101 and (b) the corresponding pore size distribution based on Dubinin−Radushkevich−Stoeckli model.

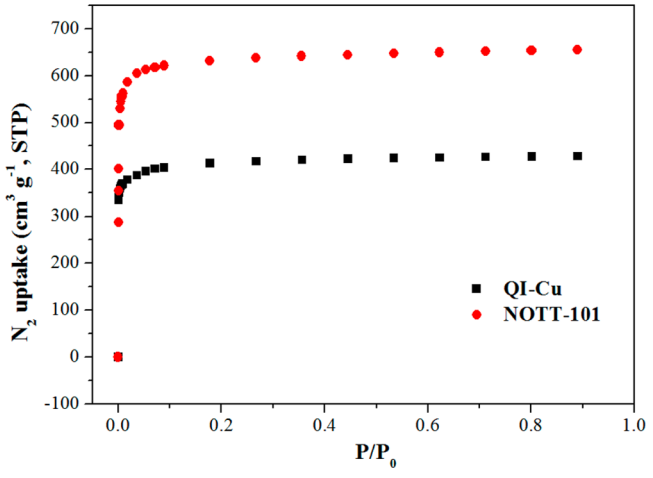

Figure 3. N_2 adsorption isotherms at 77 K for QI-Cu and NOTT-101.

3. RESULTS AND DISCUSSION

The solvothermal reaction of H_4L^2 with $Cu(NO_3)_2{\cdot}3H_2O$ in an acidic (HNO_3) mixture of H_2O/DMA (*N*,*N*-dimethylacetamide) (v/v = 1/3) at 100 °C for 3 days affords the blue, diamond-shaped crystals, solvated framework QI-Cu. The single-crystal X-ray structure and power X-ray diffraction (PXRD) results show that the framework of QI-Cu is

Table 1. Physical Parameters of QI-Cu and NOTT-101

MOFs	BET surface area[a] ($m^2\ g^{-1}$)	pore volume[a] ($cm^3\ g^{-1}$)	pore volume[b] ($cm^3\ g^{-1}$)	ref
QI-Cu	1631	0.662	0.663	this work
NOTT-101	2522	1.014	1.083	this work
NOTT-101	2247	0.886	1.083	29
NOTT-101	2805	1.080	1.083	31

[a]Calculated from N_2 isotherms. [b]Calculated from single-crystal structures with PLATON/VOID.

isostructural with NOTT-101, which is constructed from dinuclear carboxylate $[Zn_2(COOR)_4]$ SBUs and H_4L^2 ligand, exhibiting a binodal (4,4)-connected NbO type networks of $6^4 \cdot 8^2$ topology[29,30] (Figure 1). A detailed view illustrates that the NbO network consists of two types of nanocages.[30] Throughout the structure of QI-Cu, the solvent-accessible voids in its framework can be observed as 1D channels along the [100], [010], [001] and [211] direction, respectively (Figure S4, Supporting Information). However, one explicit distinction for QI-Cu and NOTT-101 lies in the size of channels due to the grafting methylol and methyl groups on the central benzene of linkers. The single-crystal structure determination of QI-Cu shows that two methylol and two methyl groups are locating on the central benzene in the linker that is perpendicular to the plane consisting of the terminal aromatic groups. To evaluate the mean pore size and have a quantitative comparison of the pore size between QI-Cu and NOTT-101, the pore size distribution (PSD) curves calculated from CO_2 adsorption isotherms at 273 K based on the Dubinin−Radushkevich−Stoeckli model[38,39] are provided, which have been successfully used for determining the narrow pore size distribution of carbon and carbon molecular sieve. As shown in Figure 2, NOTT-101 shows a wider PSD and has a peak pore size around 1.0 nm, compared with a narrower PSD and a smaller peak pore size around 0.8 nm for QI-Cu. These results suggest that the grafted methylol and methyl groups play important roles in the diminution of the pore size and the modification of the inner surface of these channels.

The nitrogen sorption isotherms were measured at 77 K to determine the specific surface areas and pore volumes of QI-Cu and NOTT-101. Prior to the measurements, the as-synthesized samples were exchanged by acetone for 1 week, during which the acetone was refreshed twice a day. Then, the acetone-exchanged samples were heat treated at 100 °C under ultrahigh vacuum for 4 h to give the fully desolvated samples. The N_2 isotherms show type-I characteristics with a plateau after P/P_0 = 0.1 (Figure 3). At P/P_0 = 0.9, the isotherm shows a N_2 uptake capacity of 428 $cm^3\ g^{-1}$ for QI-Cu and a corresponding pore volume of 0.662 $cm^3\ g^{-1}$ compared with a calculated pore volume of 0.663 $cm^3\ g^{-1}$ from single-crystal structure with PLATON/VOID (Table 1).[40] The close values indicate that the sample was almost desolvated completely. The BET surface area of QI-Cu is 1631 $m^2\ g^{-1}$, which is markedly lower than that of NOTT-101 (2522 $m^2\ g^{-1}$) (Figure S6, Supporting Information). The expected difference is the result of the free volume occupation by the incorporated methylol and methyl groups. However, importantly, the BET constant C for QI-Cu of 6842.94 is considerably greater than that for NOTT-101 of 3965.70. The constant C is commonly defined as the ratio of

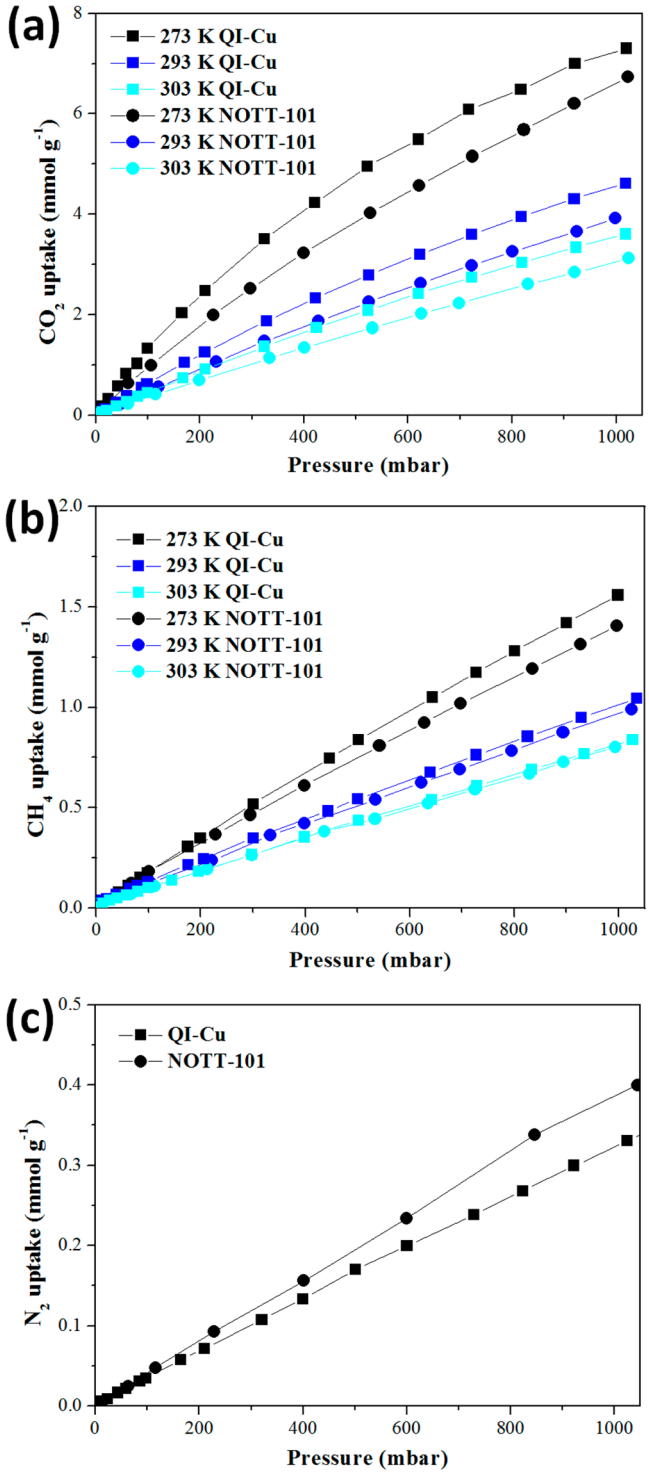

Figure 4. Adsorption isotherms of (a) CO_2 and (b) CH_4 at 273−303 K, and (c) N_2 at 293 K for QI-Cu and NOTT-101.

the molecular partition functions for molecules in the first layer, and related to the affinity of the solid with the adsorbate.[41,42] As for the framework of QI-Cu, due to the modification of methylol and methyl groups, the greater constant C precisely means stronger affinity between pore surface and guest molecules.

To investigate the gas adsorption properties, adsorption isotherms were measured for CO_2 and CH_4 adsorption on QI-Cu and NOTT-101 below 1 bar, respectively. Notably, all the

Table 2. Low-Pressure CO_2 Adsorption Capacities in Selected MOFs at 293−298 K

MOF	BET ($m^2 g^{-1}$)	Langmuir ($m^2 g^{-1}$)	pore volume ($cm^3 g^{-1}$)	uptake capacity (mmol g^{-1})	pressure (bar)	temp. (K)	ref
Mg-MOF-74	1495	1905		8.00	1	296	45
HKUST-1 (4 wt % H_2O)				6.14	1	298	46
Co-MOF-74	957	1388	0.487	5.66	1	298	47
en- MOF-74	1253			4.57	1	298	48
QI-Cu	1631	1863	0.662	4.56	1	293	this work
HKUST-1		1492		4.18	1	298	46
MPM-1-TIFSIX	840			4.00	1	298	49
NOTT-101	2522	2847	1.014	3.93	1	293	this work

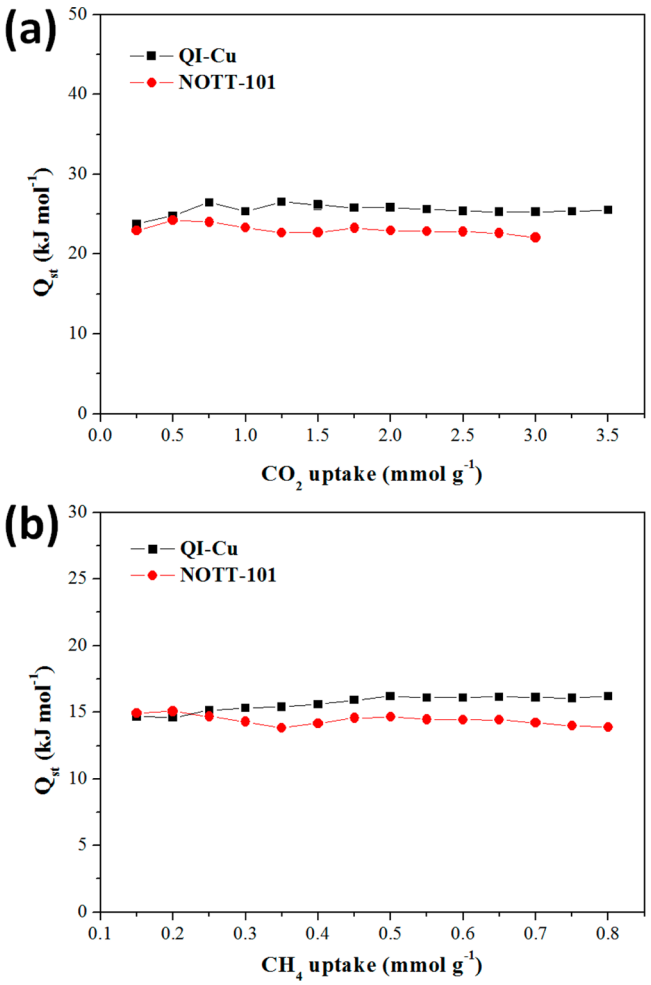

Figure 5. Isosteric heat of adsorption (Q_{st}) of (a) CO_2 and (b) CH_4 for QI-Cu and NOTT-101.

CO_2 uptake capacities for QI-Cu measured at 273−303 K were evidently larger than the corresponding capacities for NOTT-101 (Figure 4a), suggesting the significant effects of incorporated groups on increasing the gas uptake in the low pressure region. At 293 K and 1 bar, the CO_2 uptake capacity for QI-Cu was 4.56 mmol g^{-1}, which is among the top ranks of MOFs materials for CO_2 adsorption (Table 2). As for CH_4 adsorption isotherms at 273−303 K and 1 bar, similarly, QI-Cu also adsorbed more gas molecules than NOTT-101 (Figure 4b). Grand-canonical Monte Carlo (GCMC) simulation results of PCN-14, a variant of NOTT series MOFs, showed that a significant CH_4 population exists at the cage window sites.[43] As a targeted adsorbate molecule, CH_4 shows a lower adsorption strength with the adsorbent due to no polarity, dipole moment and quadrupole moment properties. Therefore, though the incorporated groups benefit the adsorption around pore windows, the weaker affinity between CH_4 and adsorbent closes the gap of uptake capacity between QI-Cu and NOTT-101. Furthermore, it is well-known that the CH_4 possesses lower isosteric heat of adsorption than CO_2, leading to the gap of uptake capacity to be disappeared gradually with the increasing of temperature. Their CH_4 uptakes come to the same value of 0.81 mmol g^{-1} at 303 K. The sorption behavior of supercritical N_2 gas at ambient temperature on MOFs materials obeys a monolayer adsorption mechanism, thereby QI-Cu and NOTT-101 both showed lower N_2 uptake capacities than CO_2 and CH_4 at 293 K and 1 bar. Moreover, in contrast to the adsorption isotherms observed for CO_2 and CH_4 uptakes, the N_2 adsorption isotherm for QI-Cu exhibited a clear descent than that of NOTT-101 (Figure 4c). It can be explained by the weaker adsorption strength for N_2 molecules, and thereby making the N_2 uptake capacity mainly determined by the pore volume over the pore environment.

The values of Virial coefficients, A_0 and A_1, reflect adsorbate−adsorbent and adsorbate−adsorbate interactions, respectively.[44] As for CO_2 and CH_4 adsorptions, A_0 for QI-Cu is less negative than NOTT-101, indicating larger host−guest affinity for QI-Cu (Table S2, Supporting Information). Furthermore, the difference of A_0 for CO_2 (−5.02042 ± 0.00320 for QI-Cu vs −5.32657 ± 0.00481 for NOTT-101) is bigger than that for CH_4 (−6.79952 ± 0.00616 for QI-Cu vs −6.84837 ± 0.00543 for NOTT-101). The results suggest that the host−guest affinity between QI-Cu and CO_2 or CH_4 is bigger than that of NOTT-101, and the difference of host−guest affinity for CO_2 is bigger than CH_4. The difference of A_0 for N_2 adsorption between QI-Cu and NOTT-101 is not significant, whereas A_1 for QI-Cu is considerably more negative than NOTT-101, indicating larger interactions between adsorbed N_2 molecules for QI-Cu due to the existing of methylol and methyl groups that do not have special affinity with N_2 molecule. Compared with CO_2 and CH_4 adsorptions, A_0 for N_2 adsorption shows less negative values, revealing the weaker host−guest affinity for N_2 which eventually leading to the lower N_2 uptake. In addition, the larger interactions between adsorbed N_2 molecules for QI-Cu result in the lower gas surface coverage and lower uptake than NOTT-101. It is evident that the Virial coefficients fully reflect the adsorption features for these MOFs materials, which is consistent with the low-pressure adsorption isotherms in Figure 4.

The isosteric heat of adsorption (Q_{st}) values below 1 bar were calculated from the CO_2 and CH_4 isotherms measured at 273−303 K upon the Clausius−Clapeyron equation (Figures 5 and S8 and S9, Supporting Information). The initial Q_{st} of CO_2

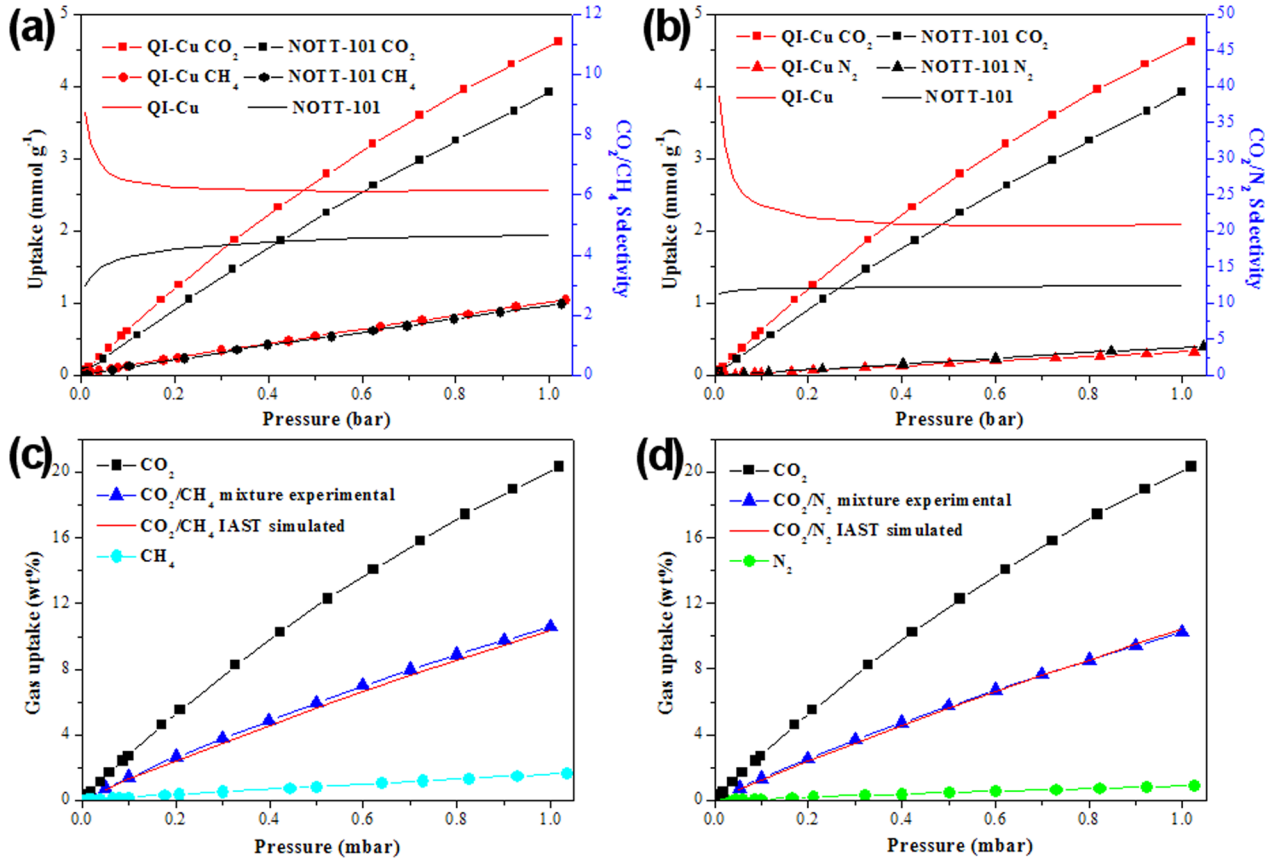

Figure 6. IAST selectivities of (a) CO_2/CH_4 and (b) CO_2/N_2 for equimolar binary gas mixtures on QI-Cu and NOTT-101, respectively. Comparisons of experimental and IAST simulated adsorption isotherms for (c) CO_2/CH_4 (42.9/57.1) and (d) CO_2/N_2 (43.3/56.7) gas mixtures at 293 K on QI-Cu.

was 23.75 ± 0.49 and 22.93 ± 0.19 kJ mol^{-1} for QI-Cu and NOTT-101, respectively, which is comparable to the previously reported values (20−35 kJ mol^{-1}).[6] Then a slight increase and a following platform can be observed with Q_{st} in the range of 25−26 kJ mol^{-1} for QI-Cu, whereas Q_{st} for NOTT-101 still remains ~23 kJ mol^{-1}. The isosteric heat of adsorption at zero coverage ($Q_{st,\ n=0}$) is a fundamental measure of the guest molecules interaction with adsorbent. The $Q_{st,\ n=0}$ for QI-Cu obtained using the Virial methods was 27.13 ± 0.45 kJ mol^{-1}, and higher than 23.56 ± 0.42 kJ mol^{-1} observed for NOTT-101 (Figures S11 and S13, Supporting Information). These results are in agreement with other works demonstrating the positive effect of incorporated methyl or hydroxy groups on CO_2 capture.[35,50,51] The higher Q_{st} for QI-Cu is attributed to the stronger affinity of pore surface toward guest molecules and the increase of the overlapping potentials for CO_2 adsorption due to the decrease in the pore size.[28,51] Similar $Q_{st,\ n=0}$ values of 14.00 ± 2.22 and 14.23 ± 0.23 kJ mol^{-1} were obtained for CH_4 on QI-Cu and NOTT-101 over the temperature range 273−303 K, respectively. However, higher Q_{st} of CH_4 for QI-Cu was observed after adsorbing small amounts of CH_4 within the range 0.25−0.8 mmol g^{-1} (Figure 5b). The Q_{st} remained stable after the initial fluctuation with a value of ~16 and ~14 kJ mol^{-1} for QI-Cu and NOTT-101, respectively. The results suggest that the incorporation of methylol and methyl groups effectively offer more active adsorption sites throughout the pores in the framework.

The studies of selective CO_2 adsorption for MOFs materials at low pressures have a profound function to the practical applications, such as removing CO_2 from flue gases. The greater isosteric heat of adsorption associated with the stronger interaction between framework and guest molecules highlights the potential improvement of adsorptive selectivity of CO_2 over other gases. To estimate the effect of linker functionalization on gas selectivity, the adsorption isotherms for CO_2, CH_4 and N_2 were measured at 293 K and 1 bar. The selectivity ratio of CO_2/CH_4 and CO_2/N_2 in QI-Cu obtained from Henry's law was 5.9/1 and 19.4/1, respectively, whereas for NOTT-101, a lower corresponding ratio of 4.6/1 and 12.4/1 was obtained (Table S4, Supporting Information). The results suggest that the incorporation of methylol and methyl groups shows great benefit not only for the enhancement of gas uptakes but also for the selectivity for CO_2 over CH_4 and N_2 in the low pressure region. In addition, ideal adsorbed solution theory (IAST)[52] is a method to predict multicomponent adsorption behaviors from single-component adsorption isotherms. As expected, the predicted adsorption selectivity of CO_2/CH_4 and CO_2/N_2 mixtures (v/v = 50/50) for QI-Cu was remarkable greater than that of NOTT-101 (CO_2/CH_4 of 6.1/1 vs 4.7/1 and CO_2/N_2 of 20.9/1 vs 12.4/1 at 1 bar) (Figure 6). To verify the accuracy of the IAST method, two additional adsorption isotherms were measured for the CO_2/CH_4 (v/v = 42.9/57.1) and CO_2/N_2 (v/v = 43.3/56.7) gas mixtures on QI-Cu, respectively. As shown in Figure 6c,d, the experimental adsorption isotherms for both of CO_2/CH_4 and CO_2/N_2 gas mixtures were in good agreement with the simulated ones by IAST calculations, clearly indicating the rationality of IAST selectivities.

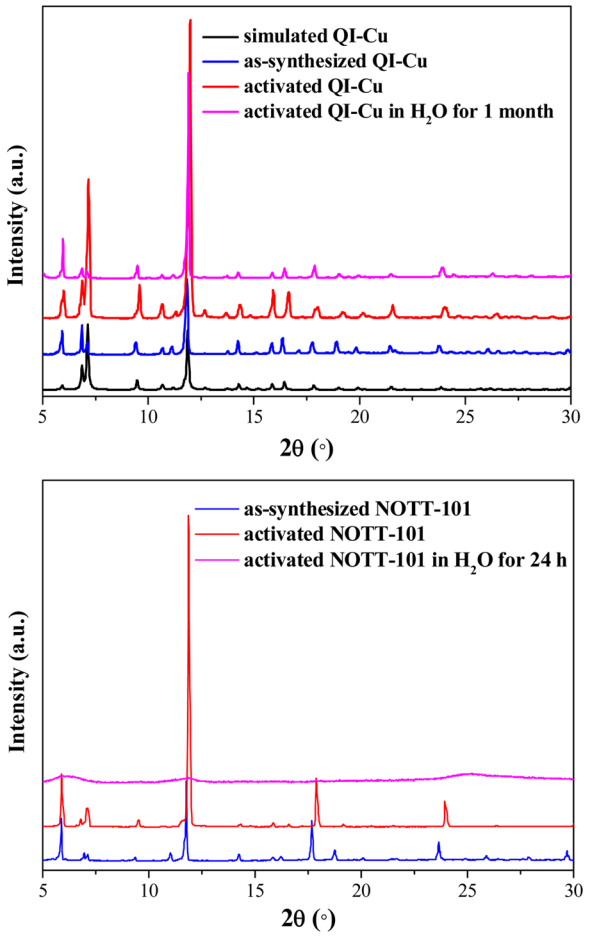

Figure 7. PXRD patterns of QI-Cu and NOTT-101. (a) Simulated (black) and experimental (blue) patterns of as-synthesized QI-Cu, experimental (red) pattern of activated QI-Cu, experimental (magenta) pattern of activated QI-Cu after being soaked in H_2O for 1 month. (b) Experimental patterns of as-synthesized (blue) and activated (red) QI-Cu, and experimental pattern of activated QI-Cu after being soaked in H_2O for 24 h (magenta).

Additionally, the viability of the sorbents in the presence of moisture plays an important role in the practical applications. Prior to the hydrostability tests, the acetone-exchanged samples were heat treated at 100 °C under ultrahigh vacuum for 4 h to give the activated samples. Then, the hydrostabilities of QI-Cu and NOTT-101 were tested in water. After the sample of QI-Cu was soaked in water for 1 month, the powder X-ray diffraction pattern of the compound remained unchanged (Figure 7a). Conversely, the sample of NOTT-101 for 24 h in water had basically collapsed because it did not show any characteristic peaks of NOTT-101 (Figure 7b). The results clearly indicate that with regard to hydrostability, QI-Cu exhibits better performance than NOTT-101. The improved hydrostability likely originated from the factor that the guest water molecules are more inclined to be adsorbed around the hydrophilic hydroxyl groups, which alleviates their unfavorable impacts on the O atoms of carboxylate. Furthermore, the grafting nonpolar methylene and methyl on the linker results in pore surface with lower surface polarization toward polar water molecules. The grafted functional groups resulting in the narrower pore windows also provide more diffusion resistance for the water molecules.

4. CONCLUSION

In conclusion, we have shown that the incorporation of methylol and methyl groups significantly enhances CO_2 uptake capacity and adsorptive selectivity of CO_2 over CH_4 and N_2 in the low pressure region for QI-Cu at room temperature. These enhancements can be attributed to the stronger interaction between framework and guest molecules by linker functionalization and the resulting higher isosteric heat of adsorption. The unexpected and outstanding hydrostability in QI-Cu also highlights that grafting nonpolar methylene and methyl on the linker may be a promising method for increasing the chemical stability and gas separation capability of MOFs.

■ ASSOCIATED CONTENT

Supporting Information

The experimental procedure, ^1H NMR spectrum, TGA profile, BET and Langmuir surface area plots, Linear Virial fitting plots, Henry's law and IAST details and crystallographic data in CIF format. CCDC 998966. This material is available free of charge via the Internet at http://pubs.acs.org.

■ AUTHOR INFORMATION

Corresponding Author

*X. B. Zhao. E-mail: zhaoxuebo@upc.edu.cn. Tel.: +86-532-80662728. Fax: +86-532-80662729.

Notes

The authors declare no competing financial interest.

■ ACKNOWLEDGMENTS

This work was supported by grants from the Natural Science Foundation of China (No. 21073216 and 21173246) and the "Hundred-talent Project" (KJCX2-YW-W34) of the Chinese Academy of Sciences for the financial support.

■ REFERENCES

(1) Pachauri, R. K.; Reisinger, A. *IPCC Fourth Assessment Report*; Intergovernmental Panel on Climate Change: Geneva, 2007.
(2) Allen, M. R.; Frame, D. J.; Huntingford, C.; Jones, C. D.; Lowe, J. A.; Meinshausen, M.; Meinshausen, N. Warming Caused by Cumulative Carbon Emissions towards the Trillionth Tonne. *Nature* **2009**, *458*, 1163−1166.
(3) Cox, P.; Stephenson, D. A Changing Climate for Prediction. *Science* **2007**, *317*, 207−208.
(4) Angamuthu, R.; Byers, P.; Lutz, M.; Spek, A. L.; Bouwman, E. Electrocatalytic CO_2 Conversion to Oxalate by a Copper Complex. *Science* **2010**, *327*, 313−315.
(5) Varghese, O. K.; Paulose, M.; LaTempa, T. J.; Grimes, C. A. High-Rate Solar Photocatalytic Conversion of CO_2 and Water Vapor to Hydrocarbon Fuels. *Nano Lett.* **2009**, *9*, 731−737.
(6) Sumida, K.; Rogow, D. L.; Mason, J. A.; McDonald, T. M.; Bloch, E. D.; Herm, Z. R.; Bae, T. H.; Long, J. R. Carbon Dioxide Capture in Metal-Organic Frameworks. *Chem. Rev.* **2012**, *112*, 724−781.
(7) Haszeldine, R. S. Carbon Capture and Storage: How Green Can Black Be? *Science* **2009**, *325*, 1647−1652.
(8) Choi, S.; Drese, J. H.; Jones, C. W. Adsorbent Materials for Carbon Dioxide Capture from Large Anthropogenic Point Sources. *ChemSusChem* **2009**, *2*, 796−854.
(9) Banerjee, R.; Phan, A.; Wang, B.; Knobler, C.; Furukawa, H.; O'Keeffe, M.; Yaghi, O. M. High-Throughput Synthesis of Zeolitic Imidazolate Frameworks and Application to CO_2 Capture. *Science* **2008**, *319*, 939−943.
(10) Rochelle, G. T. Amine Scrubbing for CO_2 Capture. *Science* **2009**, *325*, 1652−1654.

(11) Metz, B. D. O.; de Coninck, H.; Loos, M.; Meyer, L. *Special Report on Carbon Dioxide Capture and Storage*; Cambridge University Press: Cambridge, U. K., 2006.
(12) Yaghi, O. M.; O'Keeffe, M.; Ockwig, N. W.; Chae, H. K.; Eddaoudi, M.; Kim, J. Reticular Synthesis and the Design of New Materials. *Nature* **2003**, *423*, 705−714.
(13) Zhou, H. C.; Long, J. R.; Yaghi, O. M. Introduction to Metal-Organic Frameworks. *Chem. Rev.* **2012**, *112*, 673−674.
(14) Liu, J.; Thallapally, P. K.; McGrail, B. P.; Brown, D. R.; Liu, J. Progress in Adsorption-Based CO_2 Capture by Metal-Organic Frameworks. *Chem. Soc. Rev.* **2012**, *41*, 2308−2322.
(15) Li, J. R.; Kuppler, R. J.; Zhou, H. C. Selective Gas Adsorption and Separation in Metal-Organic Frameworks. *Chem. Soc. Rev.* **2009**, *38*, 1477−1504.
(16) Furukawa, H.; Ko, N.; Go, Y. B.; Aratani, N.; Choi, S. B.; Choi, E.; Yazaydin, A. O.; Snurr, R. Q.; O'Keeffe, M.; Kim, J.; Yaghi, O. M. Ultrahigh Porosity in Metal-Organic Frameworks. *Science* **2010**, *329*, 424−428.
(17) Deng, H.; Grunder, S.; Cordova, K. E.; Valente, C.; Furukawa, H.; Hmadeh, M.; Gandara, F.; Whalley, A. C.; Liu, Z.; Asahina, S.; Kazumori, H.; O'Keeffe, M.; Terasaki, O.; Stoddart, J. F.; Yaghi, O. M. Large-Pore Apertures in a Series of Metal-Organic Frameworks. *Science* **2012**, *336*, 1018−1023.
(18) Farha, O. K.; Eryazici, I.; Jeong, N. C.; Hauser, B. G.; Wilmer, C. E.; Sarjeant, A. A.; Snurr, R. Q.; Nguyen, S. T.; Yazaydin, A. O.; Hupp, J. T. Metal-Organic Framework Materials with Ultrahigh Surface Areas: Is the Sky the Limit? *J. Am. Chem. Soc.* **2012**, *134*, 15016−15021.
(19) Deng, H.; Doonan, C. J.; Furukawa, H.; Ferreira, R. B.; Towne, J.; Knobler, C. B.; Wang, B.; Yaghi, O. M. Multiple Functional Groups of Varying Ratios in Metal-Organic Frameworks. *Science* **2010**, *327*, 846−850.
(20) Wilmer, C. E.; Leaf, M.; LeeChang, C. Y.; Farha, O. K.; Hauser, B. G.; Hupp, J. T.; Snurr, R. Q. Large-Scale Screening of Hypothetical Metal-Organic Frameworks. *Nat. Chem.* **2011**, *1192*, 1−7.
(21) Yang, S.; Sun, J.; Ramirez-Cuesta, A. J.; Callear, S. K.; DavidWilliam, I. F.; Anderson, D. P.; Newby, R.; Blake, A. J.; Parker, J. E.; Tang, C. C.; Schröder, M. Selectivity and Direct Visualization of Carbon Dioxide and Sulfur Dioxide in a Decorated Porous Host. *Nat. Chem.* **2012**, *4*, 887−894.
(22) Li, J. R.; Yu, J.; Lu, W.; Sun, L. B.; Sculley, J.; Balbuena, P. B.; Zhou, H. C. Porous Materials with Pre-designed Single-Molecule Traps for CO_2 Selective Adsorption. *Nat. Commun.* **2013**, *4*, 1538.
(23) Xiang, S.; He, Y.; Zhang, Z.; Wu, H.; Zhou, W.; Krishna, R.; Chen, B. Microporous Metal-Organic Framework with Potential for Carbon Dioxide Capture at Ambient Conditions. *Nat. Commun.* **2012**, *3*, 954.
(24) Couck, S.; Denayer, J. F. M.; Baron, G. V.; Rémy, T.; Gascon, J.; Kapteijn, F. An Amine-Functionalized MIL-53 Metal−Organic Framework with Large Separation Power for CO_2 and CH_4. *J. Am. Chem. Soc.* **2009**, *131*, 6326−6327.
(25) Park, J.; Wang, Z. U.; Sun, L. B.; Chen, Y. P.; Zhou, H. C. Introduction of Functionalized Mesopores to Metal-Organic Frameworks via Metal-Ligand-Fragment Coassembly. *J. Am. Chem. Soc.* **2012**, *134*, 20110−20116.
(26) Samanta, A.; Zhao, A.; Shimizu, G. K. H.; Sarkar, P.; Gupta, R. Post-Combustion CO_2 Capture Using Solid Sorbents: A Review. *Ind. Eng. Chem. Res.* **2012**, *51*, 1438−1463.
(27) Valtchev, V.; Majano, G.; Mintova, S.; Perez-Ramirez, J. Tailored Crystalline Microporous Materials by Post-Synthesis Modification. *Chem. Soc. Rev.* **2013**, *42*, 263−290.
(28) Nugent, P.; Belmabkhout, Y.; Burd, S. D.; Cairns, A. J.; Luebke, R.; Forrest, K.; Pham, T.; Ma, S.; Space, B.; Wojtas, L.; Eddaoudi, M.; Zaworotko, M. J. Porous Materials with Optimal Adsorption Thermodynamics and Kinetics for CO_2 Separation. *Nature* **2013**, *495*, 80−84.
(29) Lin, X.; Jia, J.; Zhao, X.; Thomas, K. M.; Blake, A. J.; Walker, G. S.; Champness, N. R.; Hubberstey, P.; Schröder, M. High H_2 Adsorption by Coordination-Framework Materials. *Angew. Chem., Int. Ed.* **2006**, *45*, 7358−7364.
(30) Lin, X.; Telepeni, I.; Blake, A. J.; Dailly, A.; Brown, C. M.; Simmons, J. M.; Zoppi, M.; Walker, G. S.; Thomas, K. M.; Mays, T. J.; Hubberstey, P.; Champness, N. R.; Schröder, M. High Capacity Hydrogen Adsorption in Cu(II) Tetracarboxylate Framework Materials: The Role of Pore Size, Ligand Functionalization, and Exposed Metal Sites. *J. Am. Chem. Soc.* **2009**, *131*, 2159−2171.
(31) He, Y.; Zhou, W.; Yildirim, T.; Chen, B. A Series of Metal-Organic Frameworks with High Methane Uptake and an Empirical Equation for Predicting Methane Storage Capacity. *Energy Environ. Sci.* **2013**, *6*, 2735−2744.
(32) Makal, T. A.; Wang, X.; Zhou, H. C. Tuning the Moisture and Thermal Stability of Metal−Organic Frameworks through Incorporation of Pendant Hydrophobic Groups. *Cryst. Growth Des.* **2013**, *13*, 4760−4768.
(33) Park, J.; Wang, Z. U.; Sun, L. B.; Chen, Y. P.; Zhou, H. C. Introduction of Functionalized Mesopores to Metal−Organic Frameworks via Metal−Ligand−Fragment Coassembly. *J. Am. Chem. Soc.* **2012**, *134*, 20110−20116.
(34) Jiang, H. L.; Feng, D.; Liu, T. F.; Li, J. R.; Zhou, H. C. Pore Surface Engineering with Controlled Loadings of Functional Groups via Click Chemistry in Highly Stable Metal-Organic Frameworks. *J. Am. Chem. Soc.* **2012**, *134*, 14690−14693.
(35) Burtch, N. C.; Jasuja, H.; Dubbeldam, D.; Walton, K. S. Molecular-level Insight into Unusual Low Pressure CO_2 Affinity in Pillared Metal−Organic Frameworks. *J. Am. Chem. Soc.* **2013**, *135*, 7172−7180.
(36) Sheldrick, G. M *SHELXL-97: Program for Crystal Structure Refinement*; University of Göttingen: Germany, 1997.
(37) Sluis, P. Van Der; Spek, A. L. BYPASS: An Effective Method for the Refinement of Crystal Structures Containing Disordered Solvent Regions. *Acta Crystallogr.* **1990**, *A46*, 194−201.
(38) Carrott, P. J. M.; Carrott, M. M. L. R. Evaluation of the Stoeckli Method for the Estimation of Micropore Size Distributions of Activated Charcoal Cloths. *Carbon* **1999**, *37*, 647−656.
(39) Pinto, M. L.; Mestre, A. S.; Carvalho, A. P.; Pires, J. Comparison of Methods to Obtain Micropore Size Distributions of Carbonaceous Materials from CO_2 Adsorption Based on the Dubinin−Radushkevich Isotherm. *Ind. Eng. Chem. Res.* **2010**, *49*, 4726−4730.
(40) Spek, A. L. Single-Crystal Structure Validation with the Program PLATON. *J. Appl. Crystallogr.* **2003**, *36*, 7−13.
(41) Brunauer, S.; Emmett, P. H.; Teller, E. Adsorption of Gases in Multimolecular Layers. *J. Am. Chem. Soc.* **1938**, *60*, 309−319.
(42) Rouquerol, F.; Rouquerol, J.; Sing, K. Adsorption by Powders and Porous Solids: Principles. *Methodology and Applications*; Academic Press: San Diego, 1999.
(43) Wu, H.; Simmons, J. M.; Liu, Y.; Brown, C. M.; Wang, X.-S.; Ma, S.; Peterson, V. K.; Southon, P. D.; Kepert, C. J.; Zhou, H.-C.; Yildirim, T.; Zhou, W. Metal−Organic Frameworks with Exceptionally High Methane Uptake: Where and How is Methane Stored? *Chem.—Eur. J.* **2010**, *16*, 5205−5214.
(44) Zhao, X. B.; Xiao, B.; Fletcher, A. J.; Thomas, K. M. Hydrogen Adsorption on Functionalized Nanoporous Activated Carbons. *J. Phys. Chem. B* **2005**, *109*, 8880−8888.
(45) Caskey, S. R.; Wong-Foy, A. G.; Matzger, A. J. Dramatic Tuning of Carbon Dioxide Uptake via Metal Substitution in a Coordination Polymer with Cylindrical Pores. *J. Am. Chem. Soc.* **2008**, *130*, 10870−10871.
(46) Yazaydın, A. Ö.; Benin, A. I.; Faheem, S. A.; Jakubczak, P.; Low, J. J.; Willis, R. R.; Snurr, R. Q. Enhanced CO_2 Adsorption in Metal-Organic Frameworks via Occupation of Open-Metal Sites by Coordinated Water Molecules. *Chem. Mater.* **2009**, *21*, 1425−1430.
(47) Yazaydın, A. Ö.; Snurr, R. Q.; Park, T. H.; Koh, K.; Liu, J.; LeVan, M. D.; Benin, A. I.; Jakubczak, P.; Lanuza, M.; Galloway, D. B.; Low, J. J.; Willis, R. R. Screening of Metal−Organic Frameworks for Carbon Dioxide Capture from Flue Gas Using a Combined Experimental and Modeling Approach. *J. Am. Chem. Soc.* **2009**, *131*, 18198−18199.

(48) Lee, W. R.; Hwang, S. Y.; Ryu, D. W.; Lim, K. S.; Han, S. S.; Moon, D.; Choi, J.; Hong, C. S. Diamine-Functionalized Metal-Organic Framework: Exceptionally High CO_2 Capacities from Ambient Air and Flue Gas, Ultrafast CO_2 Uptake Rate, and Adsorption Mechanism. *Energy Environ. Sci.* **2014**, *7*, 744−751.
(49) Nugent, P. S.; Rhodus, V. L.; Pham, T.; Forrest, K.; Wojtas, L.; Space, B.; Zaworotko, M. J. A Robust Molecular Porous Material with High CO_2 Uptake and Selectivity. *J. Am. Chem. Soc.* **2013**, *135*, 10950−10953.
(50) Chen, Z.; Xiang, S.; Arman, H. D.; Mondal, J. U.; Li, P.; Zhao, D.; Chen, B. Three-Dimensional Pillar-Layered Copper(II) Metal−Organic Framework with Immobilized Functional OH Groups on Pore Surfaces for Highly Selective CO_2/CH_4 and C_2H_2/CH_4 Gas Sorption at Room Temperature. *Inorg. Chem.* **2011**, *50*, 3442−3446.
(51) Spanopoulos, I.; Xydias, P.; Malliakas, C. D.; Trikalitis, P. N. A Straight Forward Route for the Development of Metal−Organic Frameworks Functionalized with Aromatic −OH Groups: Synthesis, Characterization, and Gas (N_2, Ar, H_2, CO_2, CH_4, NH_3) Sorption Properties. *Inorg. Chem.* **2013**, *52*, 855−862.
(52) Myers, A. L.; Prausnitz, J. M. Thermodynamics of Mixed-Gas Adsorption. *AIChE J.* **1965**, *11*, 121−127.